Physics of the Earth and Planetary Interiors, 20 (1979) 134–151

CONVECTION DRIVEN DYNAMOS

A.M. SOWARD

School of Mathematics, The University, Newcastle upon Tyne, NE1 7RU (Great Britain)

(Accepted for publication in revised form April 17, 1979)

Soward, A.M., 1979. Convection driven dynamos. Phys. Earth Planet. Inter., 20: 134–151.

Various models of thermal convection in rapidly rotating fluids permeated by strong magnetic fields are discussed. Particular attention is paid to the possibility that the magnetic field can be maintained by dynamo action rather than by externally applied electric currents. Two dynamo models are given particular attention. They are the plane layer model of Childress and Soward (1972) and the annulus model of Busse (1975). Though these models do not totally resolve the geodynamo problem, they do highlight important features of hydromagnetic dynamos. As a result some speculations are made about the true character of the geodynamo.

1. Introduction

The fluid motions responsible for driving the geodynamo are generally believed to be the result of convection, thermal or otherwise. The only serious alternative is precession. Though a large amount of energy can be transmitted into the fluid by forces acting at the core surface, the recent investigations of Loper (1975) and Rochester et al. (1975) suggest that most of the available precessional energy is dissipated in boundary layers leaving an inadequate supply to drive the dynamo. On the other hand, convection maintained directly by buoyancy forces leads to motions in the main body of the core, which are likely to be sufficiently complex to regenerate magnetic field. Furthermore the wastage of energy in boundary layers is likely to be less severe. Out of all possible convective processes thermal convection is generally adopted in theoretical dynamo models (e.g. Busse, 1973, 1975; Childress and Soward, 1972) owing to its relative simplicity.

It is clear that progress towards understanding the geophysical problem can only be made through investigations of highly idealised and simplified models. Here such a model is proposed which, it is hoped, contains all the key ingredients necessary to describe qualitative features of the convection and dynamo process accurately. We shall begin by considering a self-gravitating, electrically conducting Boussinesq fluid, which is confined within a spherical container radius L and suppose that the entire system rotates rigidly with angular velocity $\mathbf{\Omega}$. Of course, the model would be more geophysically realistic if it included a central rigid core, but, since this refinement does not appear to be of fundamental importance in the ensuing dynamics, it will not be considered. We also suppose that heat sources are distributed uniformly throughout the core and as a result the temperature and corresponding density distribution are spherically symmetric. Despite the fact that the fluid is top heavy an equilibrium state of no relative motion is possible. Nevertheless once the adverse density gradient β attains a critical value β_c (say), the system becomes unstable to small perturbations. For yet larger values of β, finite amplitude convection ensues. The hope is that, for sufficiently large values of β, the convection can support a magnetic field by magnetic induction and so operate as a hydromagnetic dynamo.

Relative to coordinate axes rotating with angular velocity $\mathbf{\Omega}$, the fluid velocity $\mathbf{u}$ is governed by the

equation of motion

$$\frac{D\mathbf{u}}{Dt} + 2\boldsymbol{\Omega} \times \mathbf{u} = -\nabla p - \alpha\theta \mathbf{g} + \rho^{-1}\mathbf{j} \times \mathbf{B} + \nu\nabla^2\mathbf{u}$$

$$(\nabla \cdot \mathbf{u} = 0) \qquad (1.1a,b)$$

where ρ and p are the fluid density and pressure, $\mathbf{B}$ is the magnetic field,

$$\mathbf{j} = \mu^{-1} \nabla \times \mathbf{B} \qquad (1.1c)$$

is the electric current, μ is the magnetic permeability, α is the coefficient of expansion, $\int \boldsymbol{\beta} \cdot d\mathbf{x} + \theta$ is the temperature, $\mathbf{x}$ and t denote position and time, D/Dt is the material derivative and ν is the viscosity. The magnetic field $\mathbf{B}$ and perturbation temperature θ are governed by

$$\frac{\partial \mathbf{B}}{\partial t} = \nabla \times (\mathbf{u} \times \mathbf{B}) + \lambda\nabla^2\mathbf{B} \qquad (\nabla \cdot \mathbf{B} = 0) \qquad (1.1d,e)$$

and

$$\frac{D\theta}{Dt} = -\mathbf{u} \cdot \boldsymbol{\beta} + \kappa\nabla^2\theta \qquad (1.1f)$$

respectively, where λ and κ are the magnetic and thermal diffusivities, respectively. In addition the gravitational acceleration $\mathbf{g}$ and the temperature gradient $\boldsymbol{\beta}$ are

$$\mathbf{g} = -g_0\mathbf{x}/L, \qquad \boldsymbol{\beta} = -\beta_0\mathbf{x}/L \qquad (1.1g,h)$$

where g_0 and β_0 are their respective magnitudes at the outer boundary. The mathematical problem is completed upon specification of suitable boundary conditions. Here it is important that the condition on the magnetic field should rule out the possibility that it is maintained externally by an applied electric current.

The spherical hydromagnetic dynamo problem described above is extremely complex and only facets of the problem have been tackled so far. In this paper we will outline the two main approaches to the problem. The first approach is simply to consider convection in the presence of a prescribed magnetic field. Much of the early work on this magnetohydrodynamic convection is described by Chandrasekhar (1961). Nevertheless in Section 2 we follow Braginsky's (1964a) development as it highlights both the parameters and the physical processes which are central to the understanding of the geophysical problem. The second approach is to suppose that the convection is given and to see if there is any possibility of magnetic field regeneration. This, of course, is the kinematic dynamo problem which is now well understood (e.g. see Moffatt, 1978). When the two approaches are considered simultaneously they yield the hydromagnetic dynamo problem. In Section 3 we shall describe the plane layer hydromagnetic dynamo developed by Childress and Soward (1972). This model has had limited success and, even when the magnetic field is very weak, it suffers from the phenomenon of dynamo instability, which occurs whenever the Lorentz force aids rather than hinders convection. In Section 4 the nature of convection in a sphere is discussed both with and without an applied magnetic field. The annulus configuration developed by Busse (1970) provides a very simple but effective model for reproducing many of the important features of convection in a sphere. Busse (1975) used it as the basis of his geodynamo model and later Busse (1976) used it again with the inclusion of a zonal magnetic field to investigate the nature of convection in a sphere with magnetic field. Since the present understanding of the hydromagnetic dynamo problem is strongly influenced by the results of these two papers, the annulus model is described in detail in Section 5 together with a comprehensive discussion of the various thermal instabilities that are possible. New results are presented in Section 5.1 concerning those instabilities which can occur on intermediate length scales (see eq. 5.5a), while in Section 5.2 results which are qualitatively equivalent to some earlier results of Fearn (1979a) are outlined. Since the analysis of Section 5 contains more detail than the remaining sections, it is perhaps advisable for the non-specialist reader to bypass Sections 5.1, 5.2 initially and look instead at Figs. 2 and 3 which summarise the key results. Nevertheless we feel that the analysis in this section, none of which has appeared elsewhere, provides a useful direct extension of Busse's (1976) results. In particular they help us to assess in Section 6 the viability of his proposed weak field dynamo model together with the scaling law (see eqs. 5.9a and 6.2) for the upper limit of the strength of planetary magnetic fields. Though this model has never been worked out in complete detail, the results of Section 5 suggest that it is subject both to dynamic and dynamo instabilities. This being so the model is unlikely to operate in the manner proposed. It is therefore suggested that the geodynamo is a modified form of the

strong field model developed by Braginsky (1964b,c) with magnetic field strength of order $\sqrt{\rho\mu\lambda\Omega}$ (see eq. 2.11 below) which is intermediate between Busse and Braginsky.

2. Wave motions and convective instabilities in an unbounded fluid

Many of the important characteristics of magnetohydrodynamic convection in a rotating system can be isolated by considering an unbounded fluid, in which all conditions are uniform and $\boldsymbol{\beta}$ is parallel to $\mathbf{g}$. We, therefore, consider small perturbations

$$\mathbf{u} = \mathbf{u}', \quad \mathbf{B} = \mathbf{B}_0 + \mathbf{b}', \quad \theta = \theta', \quad p = p_0 + p' \tag{2.1}$$

of the static state and linearise eq. (1.1) accordingly. Since the resulting equations have constant coefficients, we may seek solutions proportional to

$$\exp i(\mathbf{k}\cdot\mathbf{x} - \omega t) \tag{2.2}$$

As a result the governing equations reduce to the algebraic system

$$(-i\omega + \nu a^2)\mathbf{u}' + 2\boldsymbol{\Omega}\times\mathbf{u}' =$$

$$= -i\mathbf{k}p' - \alpha\theta'\mathbf{g} + i(\rho\mu)^{-1}(\mathbf{k}\cdot\mathbf{B}_0)\mathbf{b}' \tag{2.3a}$$

$$(-i\omega + \lambda a^2)\mathbf{b}' = i(\mathbf{k}\cdot\mathbf{B}_0)\mathbf{u}' \tag{2.3b}$$

$$(-i\omega + \kappa a^2)\theta' = -\boldsymbol{\beta}\cdot\mathbf{u}' \tag{2.3c}$$

$$\mathbf{k}\cdot\mathbf{u}' = \mathbf{k}\cdot\mathbf{b}' = 0 \text{ (and } |\mathbf{k}| = a) \tag{2.3d,e}$$

which have non-trivial solutions provided

$$4\frac{(\mathbf{k}\cdot\boldsymbol{\Omega})^2}{a^2} - s^2 = \frac{-is}{-i\omega + \kappa a^2}\left(\frac{k_\perp^2}{a^2}\right)\alpha\beta g \tag{2.4a}$$

where

$$-is = -i\omega + \nu a^2 + (\rho\mu)^{-1}(\mathbf{k}\cdot\mathbf{B}_0)^2/(-i\omega + \lambda a^2) \tag{2.4b}$$

and $\mathbf{k}_\perp$ is the component of the real wave vector $\mathbf{k}$ lying in the plane perpendicular to $\boldsymbol{\beta}$ and $\mathbf{g}$. The eqs. (2.4) were first obtained by Braginsky (1964a) and following his development we now isolate some of the key magnetohydrodynamic processes.

In the absence of buoyancy forces eq. (2.4a) reduces to

$$s = \pm 2(\mathbf{k}\cdot\boldsymbol{\Omega})/a \tag{2.5}$$

and, when in addition dissipative processes are ignored, the resulting quadratic equation for ω has two roots. When the Alfven angular velocity

$$\Omega_M = B_0/L\sqrt{\rho\mu} \tag{2.6a}$$

is small compared to the rotation speed Ω

$$\Omega_M \ll \Omega \tag{2.6b}$$

as it is in the geophysically interesting case, the magnitudes of the two frequencies differ considerably. One frequency is of order Ω and corresponds to inertial waves modified by the presence of the magnetic field. The other frequency is of order Ω_{MC}, where

$$\Omega_{MC}(= \Omega_M^2/\Omega) \ll \Omega_M \tag{2.6c}$$

Unlike the fast inertial wave, the primary force balance for this slow wave is between the Lorentz (magnetic) and Coriolis forces, while the fluid inertia $\rho\partial\mathbf{u}/\partial t$ is negligible. Once the effects of dissipation are taken into account all waves decay.

With the inclusion of an adverse density gradient, the size of $\alpha\beta g$ at which instability sets in becomes our main concern. Since positive growth rates are always possible for sufficiently long vertical length scales, whenever $\alpha\beta g$ is positive, eq. (2.4) must be interpreted cautiously. For this reason, in the estimates below it is always assumed that the components of $\mathbf{k}$ in the $\mathbf{g}$, $\mathbf{B}_0$ and $\boldsymbol{\Omega}$ directions are each of order L^{-1}. Though this assumption is not always justified, it is for the cases considered in this section.

In the absence of dissipation, buoyancy (Archimedean) forces reduce the frequency ω of the slow waves, eq. (2.6c), and yield

$$\omega^2 = \left\{\frac{(\mathbf{k}\cdot\mathbf{B}_0)^2}{\rho\mu} - \left(\frac{k_\perp}{a}\right)^2\alpha\beta g\right\}\frac{(\mathbf{k}\cdot\mathbf{B}_c)^2/\rho\mu}{4(\mathbf{k}\cdot\boldsymbol{\Omega})^2/a^2} \tag{2.7a}$$

These are Braginsky's (1967) MAC waves which become unstable when ω^2 is negative and this can occur for

$$\alpha\beta g = O(\Omega_M^2) \tag{2.7b}$$

On the other hand, the fast inertial waves require much larger buoyancy forces to make them unstable. Indeed inspection of eq. (2.4) shows that the criterion corresponding to (2.7b) is

$$\alpha\beta g = O(\Omega^2) \tag{2.8}$$

Since Ω/Ω_M is large, it is reasonable to suppose that

MAC waves are more readily excited and for this reason Braginsky (1967) envisaged that they play a key role in the dynamo process.

When dissipative effects are reinstated, instability may set in through a state of either steady or oscillatory convection. The analysis of Roberts and Stewartson (1974) for a plane layer indicates clearly that the preferred mode depends mainly on the ratio

$$q = \kappa/\lambda \tag{2.9}$$

of the thermal to magnetic diffusivities. For values of q less than unity steady convection is always preferred. Therefore, as for MAC waves, viscosity is neglected and having set $\omega = 0$ in eq. (2.4) we obtain

$$\frac{k_\perp^2 \alpha\beta g}{2a^3(\mathbf{k}\cdot\boldsymbol{\Omega})\kappa} = \frac{2\rho\mu\,\lambda a(\mathbf{k}\cdot\boldsymbol{\Omega})}{(\mathbf{k}\cdot\mathbf{B}_0)^2} + \frac{(\mathbf{k}\cdot\mathbf{B}_0)^2}{2\rho\mu\,\lambda a(\mathbf{k}\cdot\boldsymbol{\Omega})} \tag{2.10}$$

This suggests that a suitable measure of the magnetic field strength and the adverse density gradient are

$$\Lambda = \Omega_{MC} L^2/\lambda (= B_0^2/\rho\mu\lambda\Omega) \tag{2.11a}$$

and

$$R = \alpha g \beta L^2/\kappa\Omega \tag{2.11b}$$

The former is the ratio of the time scales for magnetic diffusion and slow magnetic waves. The latter is a modified Rayleigh number. Evidently R is minimised and takes an order one value, when Λ is of order unity. In this case,

$$\alpha\beta g = O(E\Omega^2) \tag{2.12a}$$

where

$$E = \kappa/L^2\Omega \tag{2.12b}$$

is a modified Ekman number based on the thermal diffusivity κ.

The main deficiency in the simple calculations described above lies in the assumption that the length scale of convection is L in all directions of interest. In this respect the preferred mode is not always obliging! Often very short length scales are invoked as in the model discussed in the following section. Nevertheless the analysis does focus our attention on the three key parameters E, q, and Λ of the magnetohydrodynamic convection problem. The realised values for the geodynamo are

$$E = O(10^{-14}), \quad q = O(10^{-6}) \text{ and } \Lambda = O(3 \times 10^{-2} B_0)^2 \tag{2.13a,b,c}$$

where B_0 is measured in gauss, and for this reason it will be assumed throughout this paper that

$$E \ll 1, \quad q \leqslant 1, \quad \sigma = O(1) \tag{2.14a,b,c}$$

where $\sigma (= \nu/\kappa)$ is the Prandtl number. Whether Λ is large or small depends on the size of B_0. If B_0 is weak and takes a value of about 5 gauss appropriate to the core surface, then Λ is small, of order 10^{-2}. On the other hand, if there is a large toroidal field, say of 300 gauss, then Λ may be of order 10^2. Order one values of Λ also enjoy special significance for it is with field strengths of this size that convection can occur most readily. Indeed, according to eqs. (2.10)–(2.12) the minimum Rayleigh number R is of order unity. To compare this with the MAC wave result, eq. (2.7b) is written in the form

$$R = O(\Lambda/q) \tag{2.15}$$

Evidently, for small q, MAC waves can only be driven by density gradients with highly supercritical Rayleigh numbers.

3. Plane layer dynamo

The problem of magnetohydromagnetic convection in a rapidly rotating plane layer has been investigated by a number of authors, including Chandrasekhar (1961), Eltayeb (1972, 1975) and Roberts and Stewartson (1974). Here the particular case of a horizontal layer of fluid permeated by a horizontal magnetic field and rotating about a vertical axis will be discussed. Relative to rectangular cartesian coordinates (x, y, z), the lower boundary is $z = 0$ and

$$\boldsymbol{\Omega} = \Omega\hat{\mathbf{z}}, \quad \mathbf{g} = -g\hat{\mathbf{z}}, \quad \mathbf{B}_0 = \mathbf{B}_\perp \tag{3.1a,b,c}$$

where the superscript $\hat{}$ denotes unit vectors. For simplicity in the subsequent discussion both boundaries are assumed to be stress free and perfect conductors of both heat and electricity.

When the magnetic field is absent and the Prandtl number is greater than unity ($\sigma > 1$) instability always sets in as steady convection. The ensuing marginal convection is characterised by the temperature perturbations

$$\theta = \theta_0 \sin(\pi z/L)\, e^{i\mathbf{k}_\perp \cdot \mathbf{x}} + cc \tag{3.2}$$

where cc denotes the complex conjugate of the expression preceeding it and θ_0 is arbitrary on linear theory.

According to eq. (2.4) R and $k_\perp$ are related by

$$(k_\perp/a)^2 R = (\sigma E)^{-1}(2\pi/aL)^2 + \sigma E(aL)^4 \tag{3.3a}$$

and

$$a^2 = k_\perp^2 + \pi^2/L^2 \tag{3.3b}$$

Minimisation of R yields the critical Rayleigh number R_0 and the corresponding wave number $k_{\perp 0}$. They are given approximately by

$$R_0 = 3(4\pi^4/\sigma E)^{1/3}, \quad Lk_{\perp 0} = (\sqrt{2}\pi/\sigma E)^{1/3} \tag{3.4a,b}$$

The large values of R_0 and $k_{\perp 0}$ result because of the severe constraints imposed by the rapid rotation. Indeed to lowest order the flow is geostrophic and $\mathbf{u}$ satisfies

$$2\boldsymbol{\Omega} \times \mathbf{u} = -\nabla p \tag{3.5a}$$

The solution has the form

$$\mathbf{u} = \nabla \times \psi\hat{\mathbf{z}} + w\hat{\mathbf{z}} \tag{3.5b}$$

where ψ and w vary rapidly on the short horizontal length scale $L(\sigma E)^{1/3}$, as indicated by eq. (3.4b). At the next order of approximation the two dimensionality of the flow is broken by the competing effects of buoyancy and viscosity. Thus ψ and w vary on the relatively long vertical length scale L and are given by

$$\psi = \psi_0 \cos(\pi z/L)\, e^{i\mathbf{k}_{\perp 0}\cdot\mathbf{x}} + cc, \tag{3.6a}$$

$$w = w_0 \sin(\pi z/L)\, e^{i\mathbf{k}_{\perp 0}\cdot\mathbf{x}} + cc \tag{3.6b}$$

where

$$k_{\perp 0}\psi_0 = (\sqrt{2}/\pi)w_0, \quad \theta_0 = (\beta/\kappa k_{\perp 0}^2)w_0 \tag{3.6c,d}$$

The existence of two distinct length scales prompted Childress and Soward (1972) to use these results as the basis of a hydromagnetic dynamo model. As well as the mathematical advantages of two scales, the flow (3.5b) itself is well endowed with the helicity necessary for the dynamo process. In fact, if we define the horizontal average

$$\langle \ldots \rangle = \lim_{l\to\infty} \frac{1}{4l^2} \int_{-l}^{l}\int_{-l}^{l} \ldots \, dx\,dy \tag{3.7a}$$

then the mean value of the helicity for the convection roll described by eq. (3.6) is

$$H = \langle \mathbf{u} \cdot \nabla \times \mathbf{u} \rangle = (2^{3/2}k_{\perp 0}^2/\pi)|w_0|^2 \sin(2\pi z/L) \tag{3.7b}$$

In the dynamo models developed by Soward (1974) and Childress (1976) a non-uniform mean magnetic field

$$\mathbf{B}_0 = \mathbf{B}_\perp(z, t) \tag{3.8}$$

is considered. The magnetic field is assumed to be sufficiently weak that the motions are largely uninfluenced by the resulting Lorentz force. Consequently the flow pattern is still given by eq. (3.5), though its amplitude is as yet undetermined. It follows from dynamo theory (e.g. see Soward, 1978) that the magnetic field $\mathbf{B}_\perp$ is governed by the dynamo equation

$$\frac{\partial \mathbf{B}_\perp}{\partial t} = \nabla \times \boldsymbol{\alpha} \cdot \mathbf{B}_\perp + \lambda \nabla^2 \mathbf{B}_\perp \tag{3.9a}$$

where $\boldsymbol{\alpha}$ depends quadratically on the amplitude of the motion and

$$\boldsymbol{\alpha} \cdot \mathbf{B}_\perp = -(H/\lambda k_{\perp 0}^4)(\mathbf{k}_\perp \cdot \mathbf{B}_\perp)\mathbf{k}_\perp \tag{3.9b}$$

The single roll configuration just described is a little oversimplified. Evidently according to eqs. (3.3) and (3.4) $\mathbf{k}_\perp$ can be in any direction and so the most general motion at the onset of instability consists of the superposition of a number of rolls (say N) each corresponding to distinct $\mathbf{k}_\perp$ values. The resulting $\boldsymbol{\alpha}$-tensor is evaluated by simply summing the contribution (3.9b) from each roll separately. Of course, the success or failure of the dynamo ultimately depends on the magnitude of $\boldsymbol{\alpha}$. For this reason the finite amplitude dynamics of the system are considered and equations are derived which govern the evolution of each of the N rolls. When they are solved in conjunction with eq. (3.9), the eventual fate of the dynamo can be determined.

The presence of even a weak magnetic field leads to interesting dynamical effects. To appreciate them, it is sufficient to consider a uniform horizontal magnetic field. Thus, if we restrict attention to the critical wave number $k_{\perp 0}$ isolated in the non-magnetic problem, we see that the effect of the magnetic field is to decrease the Rayleigh number from the critical value R_0 to

$$R = R_0 \left\{ 1 - \tfrac{2}{3}(2\pi^2\sigma E)^{-1/3} \frac{(\mathbf{k}_{\perp 0} \cdot \mathbf{B}_0)^2}{\rho\mu\,\lambda\Omega k_{\perp 0}^2} \right\} \tag{3.10}$$

One important feature of this result is that the most unstable modes have wave vectors $\mathbf{k}_{\perp 0}$ aligned with $\mathbf{B}_0$. Unlike the non-magnetic case there is now a preferred mode of convection, which corresponds to rolls with

axes lying perpendicular to the magnetic field. According to eq. (3.9b) the electromotive force $\alpha \cdot \mathbf{B}_0$ resulting from these cross rolls is also in the direction $\mathbf{k}_{\perp 0}$ and so is parallel to $\mathbf{B}_0$. Consequently the magnetic field induced by the dynamo process is in the mutually perpendicular direction $\mathbf{k}_{\perp 0} \times \hat{\mathbf{z}}$. With regard to the hydromagnetic dynamo, this result is most favourable. The reason for this is that the preferred mode of convection in the presence of the non-uniform magnetic field (3.8) tends to reproduce a new magnetic field in a totally different direction. Thus as time proceeds the magnetic field and the orientation of the most vigorously convecting rolls rotate in concert about the z-axis. The sense of rotation is opposite to $\boldsymbol{\Omega}$ and proceeds on the magnetic diffusion time scale L^2/λ. The ensuing dynamo operates efficiently and should be contrasted with the kinematic case of a single roll with fixed orientation. In this latter case all solutions of eq. (3.9) decay irrespective of the roll amplitude.

Another important consequence of eq. (3.10) is that the presence of a weak magnetic field reduces the value of the critical Rayleigh number. This means that, for given Rayleigh number R close to R_0, convection becomes more vigorous as the magnetic field is intensified. Non-linear effects, however, prevent the motion from growing indefinitely. The most important of these result from the contribution

$$\langle w\theta \rangle = (2\beta/\kappa k_{\perp 0}^2)|w_0|^2 \sin(2\pi z/L) \tag{3.11}$$

to the vertical heat transport made by each individual roll. This reduces the mean vertical temperature gradient in the interior of the fluid and quickly leads to a stable finite amplitude state, in which the mean kinetic energy is constant. As indicated above, the orientation of the magnetic field rotates and so as time proceeds those rolls with $\mathbf{k}_{\perp 0}$ nearly perpendicular to the magnetic field decay. In this way roll amplitudes oscillate and the kinetic energy constraint is met.

When the mean magnetic field is weak, specifically

$$\Lambda = O(E), \tag{3.12}$$

the roll amplitudes evolve on the dynamo time scale. Soward (1974) has isolated stable hydromagnetic dynamos. On the other hand, Childress (1976) has found that for stronger magnetic fields the dynamo process is unstable despite its dynamic stability. This important conclusion can be understood in terms of model equations derived by rough order of magnitude estimates of the terms appearing in eqs. (3.9)–(3.11). Unlike Soward's weak field case the subtlties of the dynamo process do not appear to be the central issue here. Therefore we may estimate that the order of magnitude of the α-effect is simply proportional to the square of the amplitude of the velocity. In this spirit we ignore constants, ignore the details of the spatial variations and represent eq. (3.9) by

$$\frac{dB}{dt} = w^2 B - B \tag{3.13a}$$

Though we suppose that the Rayleigh number R exceeds R_0 by a small amount ΔR, the buoyancy force available to drive motions is effectively reduced by an amount proportional to ω^2 as a result of the heat transport (3.11). By contrast, eq. (3.10) indicates that the Loretnz force enhances the efficiency of the buoyancy forces by an amount which is proportional to B^2. It follows that a dynamic equilibrium is possible, in which the balance between these competing effects is represented by

$$\Delta R = w^2 - B^2 \tag{3.13b}$$

Though no quantitative conclusions should be drawn from eq. (3.13), the equations do give qualitative insight into the nature of the mechanisms at work. The two solutions of eq. (3.13) are

$$\frac{2B^2}{1-\Delta R} = \begin{cases} \exp \chi/\sinh \chi \ (t < t_0) & (3.14a) \\ \exp \chi/\cosh \chi \ (\Delta R < 1) & (3.14b) \end{cases}$$

with

$$\chi = (1 - \Delta R)(t_0 - t) \tag{3.14c}$$

where t_0 is an arbitrary constant. When $\Delta R < 1$, there is a steady finite amplitude state $B^2 = 1 - \Delta R$, $w^2 = 1$, which corresponds to $t_0 = \infty$. By contrast, when $t_0 \neq \infty$, the solutions of eq. (3.14a) grow and become infinite at time $t = t_0$, while the solutions of (3.14b) decay and tend to zero as $t \to \infty$. Consequently the finite amplitude solution is unstable to small perturbations.

The most important feature of eq. (3.14) is the demonstration that despite dynamic equilibrium the magnetic field grows in a highly non-linear fashion owing to the intense dynamo activity. This qualitative result is exhibited by Childress' full numerical study of the complete hydromagnetic dynamo problem. The result suggests that, once the magnetic field exceeds

the value specified by eq. (3.12), it will grow without bound until the Lorentz forces oppose rather than aid convection. According to eqs. (2.10) and (2.11) this is not achieved until Λ is at least of order unity.

4. Convection in a sphere

The analysis of convection in a plane layer highlights the key dynamical processes that are involved when Coriolis, buoyancy and Lorentz forces interact. In particular it shows that the critical Rayleigh number drops from an order $E^{-1/3}$ value for small magnetic fields to a minimum, when Λ is of order unity. This minimum is also a feature of the spherical convection problem formulated in Section 1. There are, however, a number of important characteristics that the plane layer model fails to reproduce.

The non-magnetic problem was first considered in detail by Roberts (1968) and Busse (1970). They found that, at the onset of instability, convection is concentrated in the neighbourhood of a cylindrical surface $C(\tilde{\omega}_0)$ located at a distance $\tilde{\omega}_0$ from the rotation axis. The reasons for localized convection are as follows. As in the case of the plane layer, the azimuthal length scale is short of order $LE^{1/3}$ with an additional dependence on the Prandtl number σ. On this length scale the flow is predominantly geostrophic and given again by eq. (3.5). Accordingly the motions tend to have the two-dimensional structure predicted by the Proudman–Taylor theorem. At the next order of approximation it becomes apparent that the component of gravity $\mathbf{g}_\perp$ normal to the rotation axis is primarily responsible for the movement of the Taylor columns. This is opposed in part by viscosity as before but also from the dependence upon the axial coordinate z over the relatively long length scale L. The latter variations are brought about by the finite slope of the boundary and this gives the sphere problem its distinctive character. The convection has the form of elongated rolls with axes parallel to the rotation axis. These rolls do not occur near the rotation axis where $\mathbf{g}_\perp$ is small neither do they occur near the equator where the axial length scale is short and the slope of the boundaries is large. Instead the rolls first appear at a radius $\tilde{\omega}_0$ which is roughly $L/2$. A distinguishing feature of marginal convection is that it takes the form of an eastward propagating wave, which closely resembles a Rossby wave. Indeed in the zero Prandtl number limit ($\sigma \to 0$) it is exactly a Rossby wave, as the effects of the buoyancy force and viscosity become vanishingly small.

The radial length scale is of order $LE^{-2/9}$ and though small it is significantly larger than the azimuthal length scale $LE^{-1/3}$. It follows that the radial structure in the vicinity of $C(\tilde{\omega}_0)$ could not be satisfactorily resolved by the low-order theories developed by Roberts (1968) and Busse (1970). For this reason Soward (1977) re-examined the problem and isolated a fundamental difficulty. It stems from the fact that the phase speed of the most unstable modes at a given distance $\tilde{\omega}$ from the rotation axis increases with $\tilde{\omega}$. Now according to our length scale estimates, we expect the wave fronts to be almost radial. Unfortunately this state of affairs cannot persist. In short, the variation of azimuthal wave speed causes the outer part of the wave front to overtake the inner part. In this way the convection rolls become highly skewed and the radial length scale shortens indefinitely. Within the framework of linear theory there appears to be no mechanism available to oppose this process and so once the radial length scale has become sufficiently short dissipative effects eventually stop the convection. Apparently only the non-linear mechanisms, which, of course, are omitted in a linear theory, can prevent the collapse of the radial length scale. The most important of these are the radial transport of heat and angular momentum. The former causes the axisymmetric part of the temperature distribution to become non-spherically symmetric. Thus the realised zonal flow consists of a contribution from the ensuing thermal wind and a contribution from the angular momentum transport. Steady solutions of the non-linear problem were found in which convection was limited in the radial extent by the destructive influence of the varying phase velocity. This effect is counteracted within the layer by the induced shears in the zonal flow.

The traditional view of the Earth's magnetic field is that inside the core it is predominantly azimuthal. This is believed to be brought about by strong zonal flows which tend to align the magnetic field with the fluid motion. If this is indeed correct it would appear reasonable to determine the effect of a zonal magnetic field on thermal convection. For these reasons Eltayeb and Kumar (1977) and more recently Fearn (1979a,b) have investigated the nature of the convection which

occurs in the presence of the magnetic field

$$\mathbf{B}_0 = B_0(\tilde{\omega}/L)\hat{\boldsymbol{\phi}} \tag{4.1}$$

where $\hat{\boldsymbol{\phi}}$ is the unit vector in the azimuthal direction. As a representative model of the Earth's magnetic field it is open to some serious criticisms. These include the fact that the meridional magnetic field is ignored and that a realistic magnetic field should be supported by electric currents flowing within the core. Indeed eq. (4.1) corresponds to a uniform axial electric current and so the current circuits must be closed outside the fluid. Despite these shortcomings the choice of (4.1) enables us to obtain some insight into the nature of thermal convection in a sphere in the presence of a magnetic field.

As the value of B_0 of the magnetic field is increased from zero the critical Rayleigh number is generally found to increase, unless the Prandtl number is large. Once Λ is of order $E^{1/3}$, the Rayleigh number begins to decrease again and drops to a minimum when Λ is of order unity (see Fig. 4). In all cases convection is oscillatory and, when $\Lambda \ll 1$, it is localised in the neighbourhood of a cylindrical surface, $c(\tilde{\omega}_0)$, whose radius $\tilde{\omega}_0$ depends on the parameters characterising the problem. The nature of the convection is essentially of two distinct types which will be described in detail in Sections 5.1.1 and 5.1.2 below. For small Λ it is manifest as a modification of the fast Rossby wave, which occurs at $\Lambda = 0$. When Λ is of order $E^{1/3}$, a transition is made to a new slow magnetic wave, which does not exist in the absence of magnetic field. Like the Rossby wave it is topographic (e.g. see Acheson, 1978) but unlike the Rossby wave neither viscosity nor inertia play a significant role. In this respect the Rossby and magnetic waves can be associated with the non-dissipative inertial and MAC waves discussed in Section 2. On the other hand, the effects of dissipation are now crucial and this is indicated clearly by the frequency of the magnetic waves, which, when $\Lambda \ll 1$, is of order $\sqrt{(\kappa\lambda)}/L_\phi^2$, where L_ϕ is the azimuthal length scale. The length L_ϕ is of order $LE^{1/3}$, when $\Lambda = O(E^{1/3})$, but increases to become of order L, when $\Lambda = O(1)$. Recently Fearn (1979a) has made a comprehensive study of the various types of solutions that can occur for various values of the diffusivity ratios q and σ. Particular attention was paid to the limiting cases of small and large q, which being particularly amenable to analytic treatment isolate clearly the important physical processes involved. It should be remarked here that many of the qualitative features of the localised convection which occurs when $\Lambda \ll 1$ are also exhibited by Busse's (1976) annulus model described in detail in the following section.

When Λ is of order unity, the oscillatory convection fills the whole sphere and a local treatment is no longer applicable. Significantly Eltayeb and Kumar (1977) and more recently Fearn (1979b) have shown that marginal convection has the character of a westward travelling wave. This feature is also exhibited by a plane layer model considered by Soward (1979a) in which the non-uniform magnetic field, eq. (4.1), is included. The analysis of this model has the advantage of simplicity and leads to a dispersion relation almost identical with eq. (2.4), which is appropriate for a uniform magnetic field. The only difference is the addition of a single term, whose origins may be traced to the magnetic hoop stress associated with magnetic field line curvature. Since convection is steady in the case of a uniform magnetic field, with $q < 1$, it is clearly the additional influence of the magnetic hoop stress that is responsible for the westward propagation of waves.

A feature of the hydromagnetic dynamo problem, which is not apparent in the case of a uniform magnetic field, is that the magnetic field itself may be unstable and drive motions. Acheson (1978) has surveyed this complicated subject and it is inappropriate for us to become deeply involved with it here. We should point out, however, that Roberts and Loper (1979), Roberts (1978), Soward (1979a) and Fearn (1979b) have stressed certain interesting relations between thermal and magnetic instabilities. They find that, in certain circumstances, the magnetic energy associated with the simple magnetic field, eq. (4.1), can be released in a rotating stably stratified system. The results of these analyses are interesting because they show clearly that the magnetic instability can be assisted rather than hindered by the density gradients associated with bottom heavy fluids.

5. The annulus model

Busse (1970) noticed that a particularly simple annulus model was capable of reproducing, qualitatively at any rate, the essential features of thermal

convection in a sphere. It is as follows. An annulus rotates with angular velocity Ω about its axis of symmetry. It has constant width DL and almost constant height L; the lower surface is horizontal while the upper surface is inclined at an angle $\tan^{-1}\eta$. The annulus is assumed to be of sufficiently large radius that the small gap approximation can be made and so curvature effects may be legitimately neglected. The system can thus be referred to local rectangular cartesian coordinates in which relative to an origin O the axes Ox, Oy, Oz are in the radial, azimuthal and axial directions, respectively. The applied temperature gradient $\boldsymbol{\beta}$ and gravity $\mathbf{g}$ are both uniform and antiparallel with Ox. The geometry of the configuration is summarised in Fig. 1.

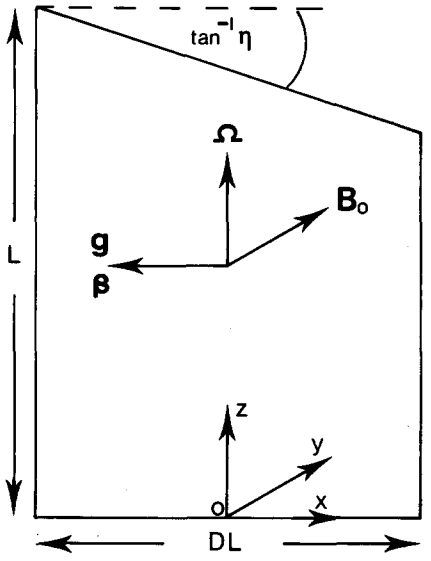

Fig. 1. A meridional cross-section of the annulus.

The reasons for the model's success stem from the remarks made in Section 4 concerning the nature of convection in a sphere. First, since marginal convection is concentrated within a cylindrical layer of width of order $E^{2/9}L$, the small gap approximation is justified with D of order $E^{2/9}$. Second, since the motion is primarily geostrophic and two dimensional, the main opposition to convection is provided by the spherical boundaries which ensure that any radial flow leads to three-dimensional motions. The effect is mimicked in the annulus by the finite slope of the top boundary. Third, since the character of the flow owes little to the axial component of gravity, it is ignored in the annulus model. Since the system imitates convection in the sphere so well, Busse (1975) adopts it as the basis of a geodynamo model.

Marginal convection in a sphere under the influence of a weak azimuthal field can also be discussed within the framework of the annulus model. In this case a uniform magnetic field $\mathbf{B}_0$ is included in the y-direction. The model, which was developed by Busse (1976), is appropriate whenever the flow is primarily geostrophic and this is generally the case, when

$$\Lambda \ll 1 \tag{5.1}$$

For order one values of Λ, the geostrophic approximation is no longer valid, convection fills the full sphere and the annulus configuration is inappropriate. When the geostrophic approximation is valid, however, the flow is given again by eq. (3.5b) to lowest order and the perturbation stream function ψ', which is almost independent of z, is governed by the z-average of the axial component of the vorticity equation. With due account taken of the vanishing of the normal velocity at $z = L$, it yields

$$\left(-\frac{\partial}{\partial t} + \nu\nabla^2\right)\nabla^2\psi' + (2\Omega\eta/L)\partial\psi'/\partial y = -\alpha g\partial\theta'/\partial y + (\rho\mu)^{-1}\mathbf{B}_0 \cdot \nabla j' \tag{5.2}$$

where $-\nabla^2\psi'$ is the axial vorticity and j' $(=\mu^{-1}\hat{z} \cdot \nabla \times \mathbf{b}')$ is the axial electric current. As in the non-magnetic problem, the radial length scale is large compared with the azimuthal length scale and so the detailed structure of the radial as well as the axial variations are incidental to the study of the stability problem. This is not the case for any dynamo action that may result, since for this fully three-dimensional motion is necessary. As our concern here is with the convection problem alone, we proceed as in Section 2 to seek solutions proportional to $\exp i(\mathbf{k} \cdot \mathbf{x} - \omega t)$, where now we set

$$\mathbf{k} = (k/L)\hat{y} \text{ and } -i\omega = \kappa P/L^2 \tag{5.3a,b}$$

The equations governing small perturbations are thus (2.3b–e), as before, while eq. (2.3a) is replaced by eq. (5.2). This leads to the cubic

$$E(P + \sigma k^2) + 2i\eta/k - R/(P + k^2) + \Lambda k^2/(qP + k^2) = 0 \tag{5.4}$$

for the dimensionless growth rate P. In order to fully appreciate the approximations that go into the annulus model, the details of eq. (5.4) should be compared carefully with those of the corresponding expression (2.4).

Busse (1976) has proposed that the geodynamo might operate when the azimuthal length scale is short compared with the size of the sphere but large compared with the length scale $E^{1/3}L$ appropriate to the onset of instability in the absence of magnetic field. In order to assess the viability of this proposal a detailed analysis is undertaken in Section 5.1 of the nature of the instabilities that can occur on this length scale. Since the wave number is restricted in this analysis the nature of the onset of instability, when disturbances of arbitrary wave length are admitted, is considered in Section 5.2. A discussion of the results is postponed until Section 6, where they can be placed in perspective relative to other convection models.

5.1. Instabilities on intermediate length scales

Since there are several different independent parameters characterising the problem, it is not surprising to find that corresponding to each of the three roots of eq. (5.4) there are a wide variety of solutions. Nevertheless, for the reasons given above, the special case

$$1 << k << E^{-1/3} \tag{5.5a}$$

is worthy of some attention. As we will see presently, it is appropriate in this parameter range to consider values of R, which are of order R_0, where

$$R_0 = Es_0^2 (>>1) \text{ and } s_0 = \eta/Ek (>>1) \tag{5.5b,c}$$

The ensuing approximations that can be made indicate the existence of two large and one small root of the cubic (5.4). The former is loosely related to Rossby waves while the latter corresponds to a magnetic wave. Both categories were mentioned in Section 4 above and will be discussed in more detail in Sections 5.1.1 and 5.1.2 below.

5.1.1. Rossby modes

The two large roots may be isolated by neglecting all terms in eq. (5.4) related to dissipative processes. Consequently, if we let

$$P = -is \tag{5.6a}$$

where s is dimensionless and measures the frequency (5.3b) in units of κ/L^2, (5.4) is given approximately by

$$-Es + 2\eta/k - (R - \Lambda k^2/q)/s = 0 \tag{5.6b}$$

and has the two roots

$$s_\pm = s_0\{1 \pm [(R_0 - R + k^2\Lambda/q)/R_0]^{1/2}\} \tag{5.6c}$$

Since instability is associated with complex values of s, it is clear that s_0 is the frequency of the modified Rossby waves which occur on the non-dissipative stability boundary

$$R = R_0 + k^2\Lambda/q \tag{5.7}$$

Above this boundary waves grow very fast on the time scale s_0^{-1}.

Whether or not the neutral waves (5.6), which exist below the boundary (5.7), grow or decay on the slow diffusion time k^{-2} depends on the small terms neglected in (5.6). To determine this small growth rate, we set

$$P = -is + p \tag{5.8a}$$

and approximate (5.4) on the basis that

$$|p/s| << 1 \tag{5.8b}$$

At leading order this gives

$$R_0(R_0 - R + k^2\Lambda/q) = \left\{(R_0 - R + k^2\Lambda/q) - \frac{(1-\sigma)k^2}{2(p+\sigma k^2)}(R - \mu k^2\Lambda/q)\right\}^2 \tag{5.8c}$$

where

$$\mu = (q^{-1} - \sigma)/(1 - \sigma) \tag{5.8d}$$

The curves of constant growth rate are parabolas all of which pass through the origin and touch the stability boundary (5.7) at its intersection with the line $R = \mu k^2\Lambda/q$ (see Fig. 2). We may also note in passing that the maximum value of Λ on the neutral parabola $p = 0$ is

$$\Lambda_1 = (R_0/k^2)q^2/(1+\sigma)(1-q) \tag{5.9a}$$

and here R and s take the values

$$R_1 = R_0(\sigma/(1+\sigma)^2 + 1/(1+\sigma)(1-q)) \tag{5.9b}$$

$$s_1 = s_0/(1+\sigma) \tag{5.9c}$$

As illustrated in Fig. 2 the unstable waves are located

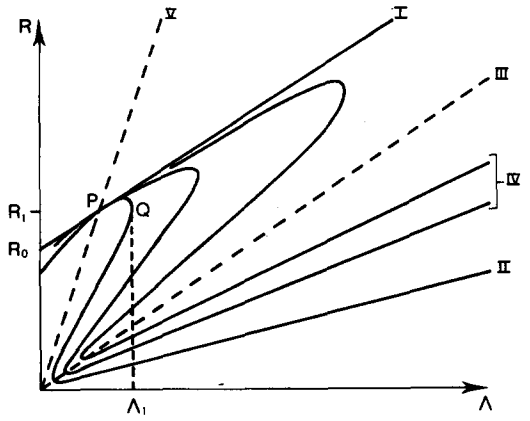

Fig. 2. The non-dissipative and dissipative stability boundaries, for fixed k, are indicated by the straight line I and curve II, respectively. The former is $R = R_0 + k^2\Lambda/q$, while the latter is a composite of eq. (5.8) with $p = 0$ and eq. (5.12) with $\tau = \tau_c$. The straight line III defined by $R = k^2\Lambda/q$ divides the region lying between the two stability boundaries into two parts. Above III the unstable waves are fast with frequency s_- (see eq. 5.5c), while below they are slow with frequency $s(\tau)$ (see eq. 5.12), where $\tau > \tau_c$. All curves of constant growth rate, typified by II and IV, pass through the point P, which lies at the intersection of I with V defined by $R = \mu k^2\Lambda/q$. Note, however, that the point P lies in the positive Λ, R quadrant only if $\mu > 0$. The point $Q(\Lambda_1, R_1)$ (see eq. 5.9) locates the maximum value of Λ, at which neutral fast waves exist.

to the right of the neutral parabola and within the strip

$$k^2\Lambda/q < R < R_0 + k^2\Lambda/q \tag{5.10}$$

The frequency of these unstable modes is s_- (>0) and so they always propagate eastward.

Now, according to eq. (5.8), the growth rate is infinite on the non-dissipative stability boundary (5.7) as well as on the line $R = k^2\Lambda/q$. Consequently the approximation $|p/s| \ll 1$, upon which eq. (5.8) is based, breaks down in the vicinity of both lines. In the case of the stability boundary (5.6), modes corresponding to eq. (5.8) with large growth rates on the resistive time scale make a transition to modes corresponding to (5.6) with small growth rates on the Rossby wave time scale. In absolute terms, of course, the growth rate increases monotonically with R. On the other hand, the nature of the instability in the vicinity of $R = k^2\Lambda/q$ will become apparent from the analysis below. For the moment it is sufficient to notice that here the frequency of the waves corresponding to s_- is very small and

$$s_- = 0 \text{ on } R = k^2\Lambda/q \tag{5.11}$$

5.1.2. Magnetic modes

So far attention has been restricted to the two large roots of eq. (5.4). To complete the picture, the nature of the remaining small root must be considered. In this limit it is reasonable to neglect the inertia term $\partial\mathbf{u}/\partial t$ as well as the viscous term in comparison with the Lorentz force. By this device we isolate the magnetic modes mentioned in Section 4. Therefore, upon setting $E = 0$ and $P = -is + p$, as before, the real and imaginary parts of the resulting quadratic lead to two equations which determine s and p in terms of Λ and R. More convenient expressions are obtained, however, if we introduce a new parameter τ. They are

$$p(\tau) = k^2\{\tau(1-q)/2q - (1+q)/2q\} \tag{5.12a}$$

$$s(\tau) = S(\tau) = s_0\{(\tau+1)R - (\tau-1)k^2\Lambda/q\}/4\tau R_0 \tag{5.12b}$$

and

$$-s(\tau)s(-\tau) = k^4\{(1-q)/2q\}^2(\tau^2 - 1) \tag{5.12c}$$

Here we regard τ as an independent variable in the definition of $S(\tau)$ but, in view of eq. (5.12c), τ, Λ and R are related in the case of $s(\tau)$. Specifically given a value of τ, substitution of (5.12b) into (5.12c) leads to a quadratic expression relating R to Λ. It defines a hyperbola with asymptotes $S(\tau) = 0$, $S(-\tau) = 0$ and has a branch in the region $\Lambda \geqslant 0, R \geqslant 0$ of interest only when

$$|\tau| \geqslant 1 \tag{5.12d}$$

From (5.12b and c) it is clear that the two hyperbolas defined by $\tau = \pm\tau_1$, where τ_1 is a given positive constant, are coincident. Consequently, everywhere on the hyperbola $|\tau| = \tau_1$, the growth rate takes one of the two values $p(\pm\tau_1)$ given by eq. (5.12a). The corresponding value of the two frequencies $s(\tau_1)$ and $s(-\tau_1)$ are determined by eq. (5.12b) and take positive and negative values, respectively, for all Λ, R on the hyperbola $\tau = \tau_c$. When $\tau = \tau_c$, where

$$\tau_1 = (1+q)/(1-q) \tag{5.13a}$$

the growth rate is zero while the corresponding frequency is

$$s = \tfrac{1}{2}s_0(R - k^2\Lambda)/R_0(1+q)\ (>0) \tag{5.13b}$$

The region of instability is defined by $\tau > \tau_c$ and here, since $s(\tau) > 0$, the unstable waves propagate eastward.

When R is of order R_0, eq. (5.12b) would suggest at first sight that that frequency s is large of order s_0. This being the case, the approximations upon which eqs. (5.12) are based would be violated. A closer inspection of (5.12b and c) reveals that for order one values of $\tau(>0$, say) the point (Λ, R) lying on the hyperbola τ = constant is close to one or other of the asymptotes

$$S(\pm\tau) = 0 \tag{5.14a}$$

where the + or − sign is taken depending on whether R is less than or greater than $k^2\Lambda/q$, respectively. In each case the realised value of the frequency $s(\pm\tau)$ at (Λ, R) is very small of order k^4/s_0 while the corresponding value of $s(\mp\tau)$ is large and given approximately by

$$s(\mp\tau) = \tfrac{1}{2}s_0(R - k^2\Lambda/q)/R_0 \tag{5.14b}$$

In general only the low-frequency solution is admissible and this supplements the two solutions (5.6c) found earlier. On the other hand, when R and $k^2\Lambda/q$ are small compared with R_0, both the solutions $s(\pm\tau)$ of (5.12) are acceptable. Indeed, when $R > k^2\Lambda/q$, (5.14b) now approximates not just $s(-\tau)$ but also s_- in (5.6c).

When

$$|k^2\Lambda/qR - 1| \ll 1 \quad (R = O(R_0)) \tag{5.15}$$

the approximations leading to eq. (5.14) fail and the complete shape of the hyperbolas must be considered. In this region, eq. (5.12) indicates that in addition to $k^2\tau$ both $s(\tau)$ and $s(-\tau)$ are of order $ks_0^{1/2}$ and though large they are still small compared with s_0. Therefore, both solutions are acceptable and provide the key to our understanding of the switch over from magnetic to Rossby modes that occurs across the line $R = k^2\Lambda/q$. In particular we may note that, when $R = k^2\Lambda/q$, the frequency and the growth rate of the growing mode are both given by

$$s = p = \tfrac{1}{2}\left(\frac{1-q}{q}\,\frac{R}{R_0}\right)^{1/2} ks_0^{1/2} \tag{5.16}$$

The general picture, which emerges and is summarised in Fig. 2, is the following. Consider a fixed value of Λ with $k^2\Lambda/q$ of order R_0. All modes are stable below the asymptote $S(\tau_c) = 0$, namely the line $R = k^2\Lambda$. Above this line the slow magnetic modes defined by eq. (5.12) with $\tau = \tau_0$ are unstable. Their frequencies and growth rates are of order k^4/s_0 and k^2, respectively. Across the line $R = k^2\Lambda/q$, the growing magnetic modes make a rapid transition to the growing Rossby modes defined by s_- in eq. (5.6c). The frequencies are now of order s_0 but the growth rates remain the same, of order k^2. Other than the rapid frequency change the most striking feature of the transition is the relatively large growth rates of order $ks_0^{1/2}$ which are achieved (see eq. 5.16). Once above the non-dissipative stability boundary both s and p are of order s_0.

5.2. The onset of instability

In Section 5.1 above, attention was restricted to fixed values of the wave number k. When the critical Rayleigh number is obtained without any special restrictions on k, a rather different picture emerges. First, in the absence of dissipation, minimisation of R, as given by eq. (5.7), R with respect to k yields the critical Rayleigh number

$$R_c = 2\eta(\Lambda/Eq)^{1/2} \tag{5.17}$$

Second, when the effects of dissipation are included, the true critical Rayleigh number is obtained by minimising R, as given by eq. (5.4), with respect to k, keeping $s(=iP)$ real. Fearn (1979a) has undertaken a similar analysis within the broader context of convection in the sphere. We will outline below all his main conclusions, which relate to our simpler problem, but will derive the results for the annulus model using a technique which we believe is new in the context of stability theory.

We begin by introducing the physically relevant parameters

$$X = k^2/s \text{ and } Y = (1+\sigma)^{-1}(s_0/s) \tag{5.18a,b}$$

whose magnitudes measure the ratio of the oscillation time scale to the diffusion and Rossby wave time scales, respectively. In terms of these new variables the real and imaginary parts of eq. (5.4) determine the following parametric representations of Λ and R. They are

$$\Lambda = 2[E(1+\sigma)\eta^2]^{1/3}\hat{\Lambda}, \quad R = 2[\eta^4/E(1+\sigma)]^{1/3}\hat{R} \tag{5.19a,b}$$

where

$$\hat{\Lambda} = (1-q)^{-1}(Y-\tfrac{1}{2})(q^2+X^2)(X^2Y)^{-2/3}, \qquad (5.19c)$$

$$\hat{R} = (1-q)^{-1}\left(Y-\frac{1}{2}+\frac{\epsilon}{2}\right)(1+X^2)(XY^2)^{-2/3} \qquad (5.19d)$$

and

$$\epsilon = (1-q)\sigma/(1+\sigma) \qquad (5.19e)$$

By varying X and $Y(\geqslant\frac{1}{2})$ a region in the $\hat{\Lambda}, \hat{R}$ plane is generated. Its lower edge defines the stability boundary and the value of $\hat{R}$ here for a particular choice of $\hat{\Lambda}$ determines the critical Rayleigh number. On this boundary and on some other curves, which are of no particular interest, the Jacobian $\partial(\hat{\Lambda}, \hat{R})/\partial(X, Y)$ vanishes. Application of this condition yields

$$F(Y, \epsilon) = G(X^2, q^2) \qquad (5.20a)$$

where

$$F(Y, \epsilon) = -\frac{(2Y-1)(Y-2+2\epsilon)}{(2Y-1+\epsilon)(Y+1)} \qquad (5.20b)$$

$$G(X^2, q^2) = \frac{(X^2+q^2)(2X^2-1)}{(X^2+1)(X^2-2q^2)} \qquad (5.20c)$$

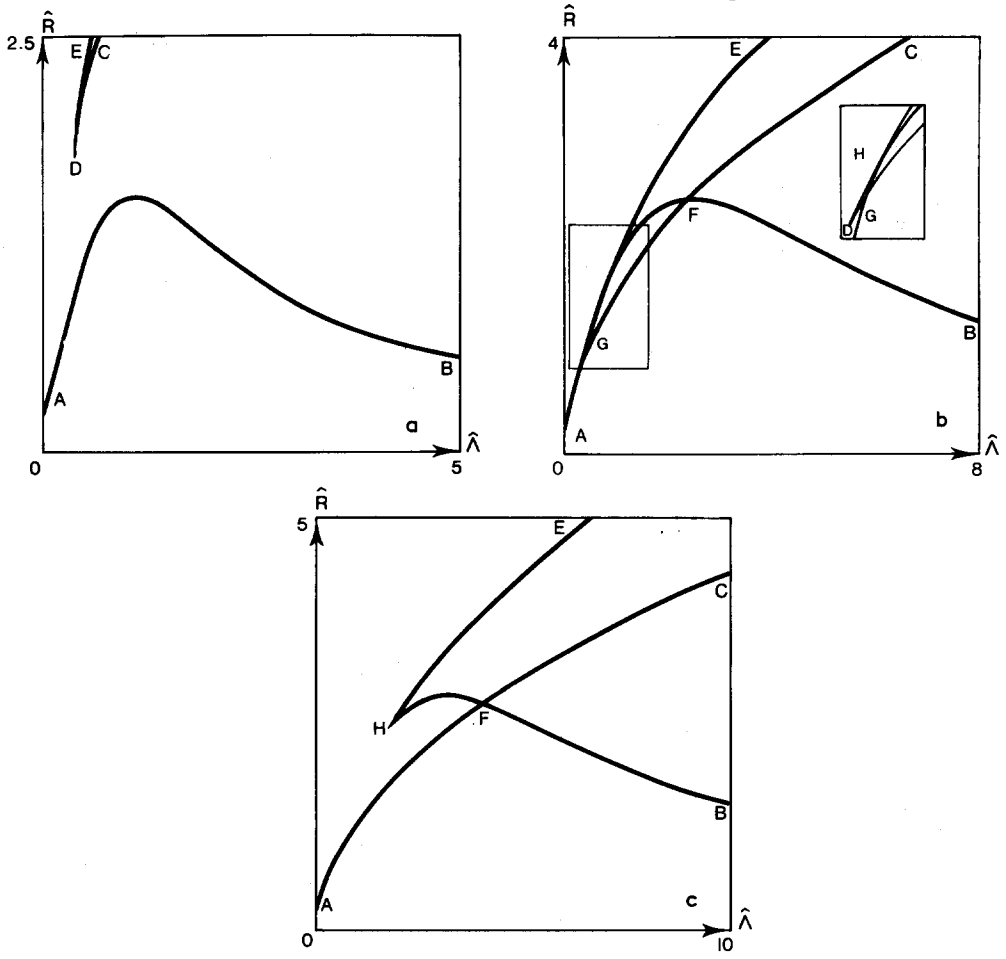

Fig. 3. With $\sigma = 0.1$, $\hat{R}$ is plotted vs. $\hat{\Lambda}$ for various values of q according to eqs. (5.19) and (5.20). The stability boundary corresponds to the continuous curve AB in (a) $q_{top} > q = 0.25$; the segmented curves AG, GF, FB in (b) $q = q_{top} = 0.53135\ldots$; the segmented curves AF, FB in (c) $q_{top} < q$ 0.6. (The insert in (b) which is not drawn to scale provides a blow up of the curves near G and illustrates how reconnection takes place at H.) The values of X^2 and Y appropriate to the asymptotic behaviour at B, E and C are described in the caption to Fig. 5 while at B, $\hat{R} = 1/\hat{\Lambda}$, and at E and C, $R \propto \hat{\Lambda}^{1/2}$ (see also eqs. 5.21–5.23).

The various solutions of eqs. (5.19) and (5.20) are discussed in detail in the Appendix. It transpires that three separate cases can be distinguished and they are illustrated in Fig. 3 for $\sigma = 0.1$. The results indicate that the stability boundary is smooth for $q \leqslant q_1$ (see curve AB in Fig. 3a), has two slope discontinuities at F and G for $q_1 < q < q_2$ (see Fig. 3b) and has one slope discontinuity at F for $q_2 \leqslant q < 1$ (see Fig. 3c). The values of q_1 and q_2 depend on σ. At F and G two solution curves of eqs. (5.19) and (5.20) intersect yielding two distinct modes each with different values of X^2 and Y but each with the same Rayleigh number. It follows that the modal dependence upon $\hat{\Lambda}$ is continuous, when $q \leqslant q_1$, has two discontinuities at F and G, when $q_1 < q < q_2$, and only one discontinuity at F, when $q_2 \leqslant q < 1$.

The most striking features of the stability boundary are illustrated by the case

$$\sigma \ll 1, q \ll 1 \qquad (5.21a,b)$$

In this limit the curve AB is approximated by

$$\hat{R} = \begin{cases} \hat{\Lambda}(3 - 2\hat{\Lambda}) & (0 < \hat{\Lambda} \leqslant 1) \qquad (5.22a) \\ 1/\hat{\Lambda} & (1 \leqslant \hat{\Lambda}) \qquad (5.22b) \end{cases}$$

while the curve DC of Fig. 3(a), (b) is approximated by

$$\hat{R} = (\sqrt{8\epsilon}/q)\hat{\Lambda}^{1/2} \qquad (5.23)$$

We consider first the case

$$q < 4\sqrt{\epsilon} \qquad (5.24)$$

for which the curve DC is above AB, and we have smooth modal dependence on $\hat{\Lambda}$. When $0 < \hat{\Lambda} < 1$, both X and Y are of order unity and so the Rossby and diffusion time scales cannot be distinguished. Therefore convection is not strictly of the type considered in Section 5.1.1. On the other hand, it is clearly the extention of the non-magnetic convection, which occurs when $\sigma \ll 1$, and this is of the Rossby mode type. Consequently, we describe the convection in the range $0 < \hat{\Lambda} < 1$ as modified Rossby waves, which all have the same phase speed

$$s/k = (\eta/E)^{1/3} \qquad (5.25)$$

since $X^2 Y \doteqdot 1$. In the neighbourhood of $\hat{\Lambda} = 1$ the character of the mode changes abruptly and when $\hat{\Lambda} > 1$, X and Y are of order $q^{1/2}$ and q^{-1}, respectively. Again referring to eq. (5.18) this shows that the time scale of oscillation is long compared with the Rossby time scale s^{-1} and therefore convection corresponds to the slow magnetic mode discussed in Section 5.1.2. It should be emphasised that the sudden transition from Rossby to magnetic modes that occurs at $\hat{\Lambda} = 1$ is peculiar to the case $q \ll 1$. For the cases illustrated in Fig. 3, the transition is continuous. Finally we consider briefly the case

$$q > 4\sqrt{\epsilon} \qquad (5.26)$$

Now the curve DC intersects AB at the two points G and F of Fig. 3(b). On the segment GF, X is of order q^3 and Y is approximately 1/2. The corresponding convection is clearly described as a Rossby mode.

As stated earlier the character of the three different types of solution described above was determined earlier by Fearn (1979a). He was primarily concerned, however, with the behaviour of the critical Rayleigh number for the full sphere. In that case there is an added degree of flexibility owing to the arbitrariness of the radius $\tilde{\omega}_0$ of the circular cylinder close to which convection takes place. The annulus model considered above represents the special case in which that radius is held fixed and for this reason must be interpreted cautiously. Nevertheless, though some features of the convection in a sphere cannot be illustrated without allowing for variations in $\tilde{\omega}_0$, there are some features which are duplicated. These include the modal discontinuity at F (see Fig. 3c) which is found to be very common, as well as the smooth dependence on Λ (see Fig. 3a) which also occurs, but less often. On the other hand, Fearn (1979a) found no examples with the modal discontinuity associated with the point G in Fig. 3(b) except when the variations of $\tilde{\omega}_0$ are restricted as they would be if the presence of a central rigid core is allowed for.

6. Discussion

Busse's (1975) original geodynamo model based on the annulus configuration of Section 5 was developed through perturbations about the non-magnetic system. As in the case of the plane layer dynamo discussed in Section 3 the Rayleigh number is assumed to be slightly in excess of the critical value appropriate to the non-magnetic problem. Provided the excess is suf-

ficiently large, finite amplitude convection ensues capable of sustaining large-scale magnetic field. The magnitude of this field is exactly that required to prevent any further intensification of the convection. Like the plane layer model it is dynamically stable but unlike the plane layer model the dynamo process itself is also stable.

The success of the annulus model pivots on the fact that, near $\Lambda = 0$, the critical Rayleigh number R_c is an increasing function of Λ. This is only the case, however, when $\Lambda \leqslant O(E^{1/3})$ (see eq. 5.19 and Fig. 3). For larger values of Λ, R_c is a decreasing function and only begins to increase again, when $\Lambda = O(1)$ (e.g. see eqs. 2.10 and 2.11). Within the interval $E^{1/3} << \Lambda << 1$, the results for the plane layer would suggest, therefore, that the dynamo process would be unstable. Nevertheless, Busse (1976, 1978a,b) has proposed that the geodyanmo operates precisely within this range and bases his arguments on the neutral curve II in Fig. 2. He argues that the dynamo is an extension of the weak field model described above, existing only in the vicinity of the upper section of the Rossby mode branch of curve II. He, therefore, suggests that the magnetic field grows to the largest admissible value on this section of the curve, namely Λ_1, defined by eq. (5.9a), which is equivalent to Busse (1976, eq. 26). The Rayleigh number appropriate to this neutral wave is given by eq. (5.9b), which may be written independently of k in the alternative form

$$R_1 = C\eta(\Lambda/Eq^2)^{1/2} \tag{6.1}$$

where the constant of proportionality C is of order unity for $q < 1$. Using the estimates, eq. (2.13), of q and E together with Busse's estimates

$$\eta = 1/\sqrt{3}, \quad \sigma = O(10^{-1}), \quad k = O(10) \tag{6.2a}$$

appropriate to the Earth's core, eq. (5.9a) yields

$$\Lambda_1 = O(10^{-1}) \tag{6.2b}$$

Such an estimate is not unreasonable and indicates the existence of a weak magnetic field comparable in size with its surface value.

The viability of Busse's proposals hinge on two questions. First, is the dynamo stable? Second, is the system dynamically stable? To answer the first question, consider Fig. 2. Suppose that the dynamo is operating close to $Q(\Lambda_1, R_1)$. Then it is clear that if Λ increases the amplitude of the Rossby waves is likely

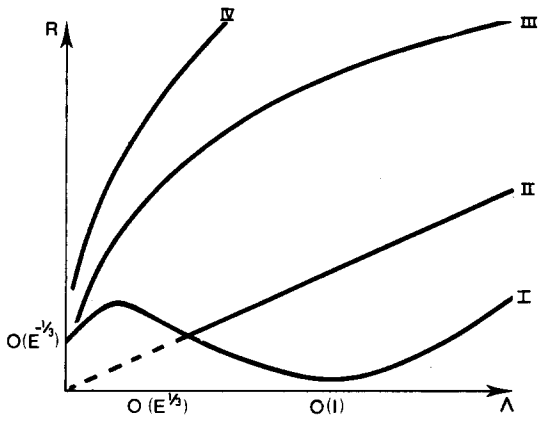

Fig. 4. A qualitative sketch of the important stability boundaries, isolated in the text. The critical Rayleigh number for the onset of instability within a sphere for the magnetic field (eq. 4.1) is indicated by curve I. The section of I, for which $\Lambda << 1$, is also given in Fig. 3 from the results of the annulus model. MAC waves occur in the vicinity of the straight line II, given by $R \propto \Lambda/q$ (see eq. 2.7a). The non-dissipative stability boundary for Rossby waves is indicated by the parabolic arc III (see eq. 5.17). As k varies the point Q in Fig. 2 also marks out a parabolic arc (see eq. 6.1); this is indicated by the curve IV.

to be intensified rather than suppressed. Under these conditions the dynamo is likely to be unstable, as pointed out in Section 4. To answer the second question, we consider the size of R_1, given by eq. (6.1), at Q. The ratio of R_1 to the critical Rayleigh number $R_c(\propto 1/\Lambda)$ is enormous (see also Fig. 4). Indeed R_1 is even an order of magnitude $q^{-1/2}$ larger than the critical value, eq. (5.17), derived when dissipation was ignored! It is therefore most unlikely that the neutral mode of convection defined by Q_1, which is basically difficult to excite, should persist and not be unstable to more favourable modes of convection. We therefore suggest that the system is dynamically unstable. We make these remarks with slight reservation because the system envisaged by Busse (1976, 1978a,b,c) is fully non-linear, whereas the theory that has been developed is only quasi-linear. The criticisms we have put forward are directed at the quasi-linear theory, upon which the importance of Λ_1 is based, and whether or not they are applicable to a non-linear theory, which remains unspecified, is not clear.

What alternatives are there to Busse's proposals? One is simply that Λ is of order unity and that the Rayleigh number is also close to its order one critical

value R_c. Here dynamo stability should be achieved because R_c is an increasing function of Λ, when $\Lambda \geqslant$ O(1). In addition, the system should also be dynamically stable because the Rayleigh number is close to R_c. This picture, which again pivots on a quasi-linear theory, is far too simplistic and cannot work. To highlight the difficulty, we note that for dynamo action the magnetic Reynolds number

$$R_\lambda = UL/\lambda \tag{6.3a}$$

based on a typical fluid velocity U must be at least of order unity and so the Peclet number

$$R_\kappa = UL/\kappa \tag{6.3b}$$

must be at least of order q^{-1}. It follows that convection must be highly non-linear and to obtain flows of the required intensity we may anticipate that the Rayleigh number must be well in excess of its critical value. Since the intense non-linear effects are largely concentrated in promoting heat transport, the mean temperature profile must be maintained at a value very close indeed to the adiabat and this makes the realised value of the Rayleigh number a very uncertain quantity. By contrast, this is not the case for the proposed order one value of Λ, which is based on an anticipated balance of the Coriolis and Lorentz forces. Here since the diffusivity ratio q is so small, the relative sizes of the two forces are unlikely to be significantly altered by non-linear processes.

Little is known about the non-linear convection problem. Roberts and Stewartson (1974, 1975), however, have initiated the study of non-linear convection in the presence of a uniform horizontal magnetic field $\mathbf{B}_0 = B_0\hat{\mathbf{y}}$ in the simple plane layer geometry of Section 3. The analysis hinges on the fact that, when viscosity is neglected, there is a non-convective geostrophic mode with velocity $U(x)\hat{\mathbf{y}}$ which suffers no damping. This mode though not excited by buoyancy forces is readily driven by the Lorentz force, when the uniform magnetic field is modified by the finite amplitude convection. When $\Lambda > \sqrt{3}$, two modes of convection are possible, which consist of rolls with axes oblique but making equal angles with the magnetic field. Roberts and Stewartson find that there exist finite amplitude equilibria in which only one family of rolls is present. They also find that, for certain values of Λ, the equilibria are unstable to perturbations composed of the second set of rolls together with the shear flow $U(x)$. In this case no stable finite equilibria were found. A more recent extension by Soward (1979b), which is restricted to $q \ll 1$, isolated stable equilibria, when the damping of the shear flow $U(x)$ by Ekman suction is taken into account. It was shown, however, that as the Rayleigh number is increased above its critical value, the geostrophic flow $U(x)$ quickly becomes large compared with the convective velocities. The result suggests that, for Rayleigh numbers well above their critical values, fluid motions within a sphere will be dominated by large zonal flows with relatively small asymmetric convective motions, while the magnetic field itself is largely zonal.

The magnetic field and flow configuration just described is, of course, very similar to that proposed by Braginsky (1964b,c, 1967). The main difference between the two pictures is that whereas Braginsky envisages convection in the form of non-dissipative MAC waves, we envisage that diffusion plays a central part in the convective process. The reason is simply that, when Λ = O(1), the MAC waves and the magnetic diffusion time scales are comparable (see eq. 2.11a). The ensuing dynamo is still of the $\alpha\omega$-type but the α-effect is not that appropriate to the high-conductivity limit. Instead it more closely resembles the low-conductivity limit of the annulus and plane layer models. In conclusion we suggest that the geodynamo operates with Λ = O(1) or slightly larger and R = $O(q^{-1})$, roughly at the location of Braginsky's MAC waves. Here motion should be sufficiently intense to regenerate magnetic field and perhaps conditions are also favourable for dynamo stability.

Acknowledgement

The author would like to thank Dr. D. Fearn for many useful discussions relating particularly to Section 5.

Appendix

In order to distinguish the various types of solutions of eqs. (5.19) and (5.20) that can occur it is necessary to appreciate the character of the functions F and G. When $Y = \frac{1}{2}$, F is zero and as Y increases F reaches a maximum $F_{max}(\epsilon)(<1-\epsilon)$ at $Y = Y_{max}(\epsilon)$ (say). It then decreases and approaches -1, as $Y \to \infty$ (see Fig.

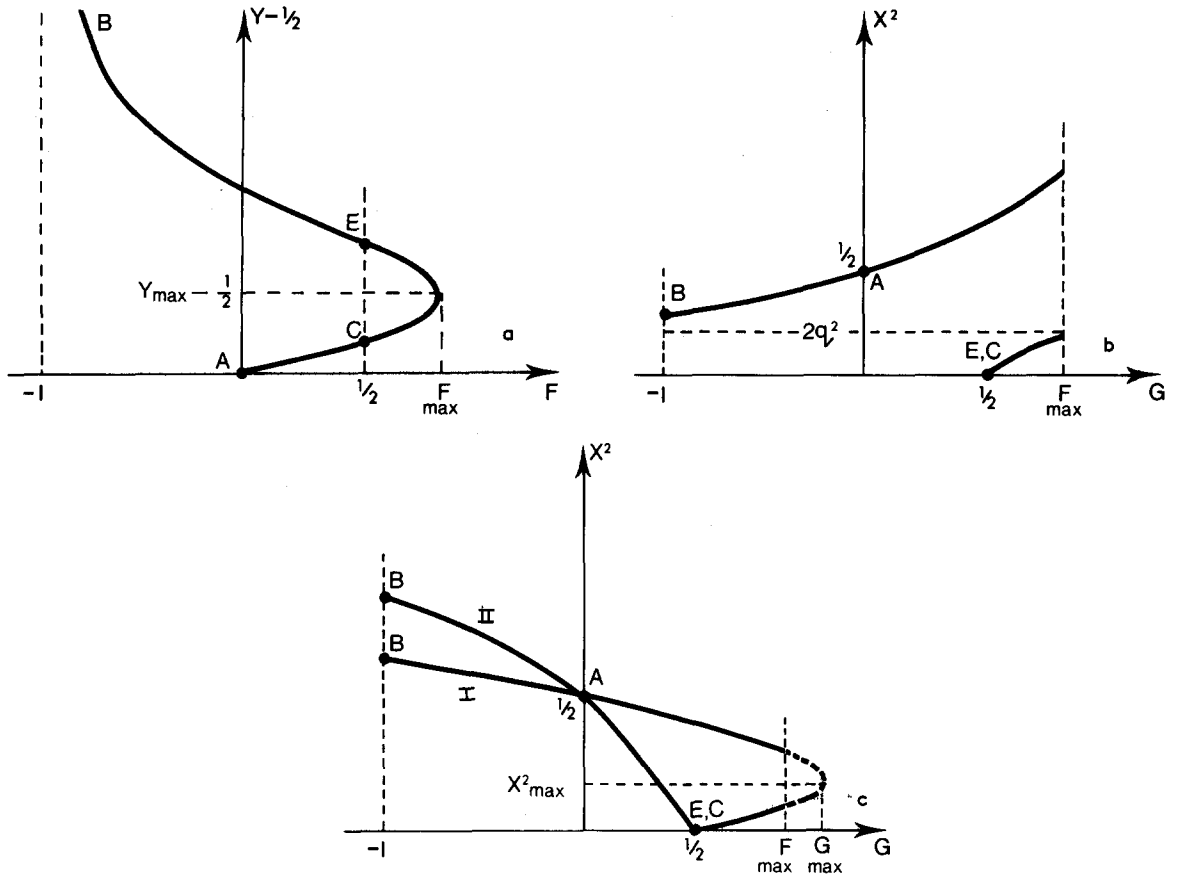

Fig. 5. F and G are plotted vs. $Y - \frac{1}{2}$ and X^2, respectively, for various values of ϵ and q. The points labelled A, B, C, E relate to the asymptotic behaviour illustrated by the plots of $\hat{R}$ vs. $\hat{\Lambda}$ in Fig. 3. The values of (X^2, Y), which define the points, are $(\frac{1}{2}, \frac{1}{2})$ at A, (q, ∞) at B, $(\frac{1}{2}, Y_C)$ at C and $(\frac{1}{2}, Y_E)$ at E where $Y_C < Y_{max} < Y_E$. (a) $\epsilon < \frac{1}{9}$. (b) $0 < q < \frac{1}{2}$. (c) Curves I and II illustrate the cases $\frac{1}{2} < q < q_{top}$ and $1/\sqrt{2} < q < 1$, respectively.

5a). The function G is more complicated and three distinct cases may be distinguished, which are illustrated in Fig. 5(b), (c). When $q < \frac{1}{2}$, G is $\frac{1}{2}$ at $X^2 = 0$ and increases to $+\infty$ as $X^2 \uparrow 2q^2$. On the other hand, G is 2 at $X^2 = \infty$ and decreases to $-\infty$ as $X^2 \downarrow 2q^2$. When $\frac{1}{2} < q < 1/\sqrt{2}$, G increases from $\frac{1}{2}$ at $X^2 = 0$ to a maximum value

$$G_{max}(q^2) = (\gamma - \sqrt{\gamma^2 - 1})^2 (<1) \quad (\gamma = 3q/(2q^2 + 1)) \tag{A1a}$$

at

$$X^2_{max}(q^2) = q[(2G_{max} - 1)/(2 - G_{max})]^{1/2} \tag{A1b}$$

It then decreases and approaches $-\infty$ as $X^2 \uparrow 2q^2$. For $X^2 > 2q^2$, we have $G > 1 > F_{max}(\epsilon)$ implying that eq. (5.20a) has no solutions. The character of G in this region is therefore of no interest. The case $1/\sqrt{2} < q < 1$ is the same as the previous case except that there is no local maximum. Instead F decreases throughout the interval $0 \leqslant X^2 \leqslant 2q^2$.

When $\epsilon > 1/9$, or equivalently

$$q < (8\sigma - 1)/9\sigma \quad (<1) \tag{A2}$$

F_{max} is less than $\frac{1}{2}$ and so X is determined by eq. (5.20) as a single-valued function of Y. Consequently eq. (5.19c,d) determines a single curve in the $\hat{\Lambda}, \hat{R}$ plane, similar to AB in Fig. 3(a), which marks the stability boundary.

When $\epsilon < 1/9$, or equivalently

$$(8\sigma - 1)/9\sigma < q < 1 \tag{A3}$$

eqs. (5.19c,d) and (5.20) determine two distinct curves in the $\hat{\Lambda}, \hat{R}$ plane. One is generally smooth, the other has a cusp (see Fig. 3) while their topology, for fixed σ, depends upon whether q is less than or greater than the value q_{top} at which $F_{max} = G_{max}$. Unlike the case (A2), $\hat{R}$ is not a single-valued function of $\hat{\Lambda}$ and so here only the smallest value actually determines the critical Rayleigh number. Three distinct cases are possible, all of which may be illustrated with $\sigma = 0.1$ and $0 \leqslant q < 1$ (see Fig. 3). As q is increased from zero the curve EDC lies totally above AB (see Fig. 3a). When $q = q_1$ (say), the curve DC touches AB and, for larger values of q, DC intersects AB at the two points G and F. When $q = q_{top}$, the curve AB touches DE at H (see Fig. 3b) and for larger values of q the curves at H reconnect leaving the two distinct curves EHB and AHDC. When $q = q_2$ (say) the two cusps at H and D coincide with G and evaporate. For larger values of q the curve AC is smooth as illustrated in Fig. 3(c).

References

Acheson, D.J., 1978. Magnetohydrodynamic waves and instabilities in rotating fluids. In: P.H. Roberts and A.M. Soward (Editors), Rotating Fluids in Geophysics, Academic Press, London, pp. 315–349.

Braginsky, S.I., 1964a. Magnetohydrodynamics of the Earth's core. Geomagn. Aeron. (USSR), 5: 898. Translated in Geomagn. Aeron., 5: 698–712 (1965).

Braginsky, S.I., 1964b. Self-excitation of a magnetic field during the motion of a highly conducting fluid. Zh. Eksp. Teor. Fiz., 47: 1084. Translated in Soviet Phys. J.E.T.P., 20: 726–735 (1965).

Braginsky, S.I., 1964c. Theory of the hydromagnetic dynamo. Zh. Eksp. Teor. Fiz., 47: 2178. Translated in Soviet Phys. J.E.T.P., 20: 1462–1471 (1965).

Braginsky, S.I., 1967. Magnetic waves in the Earth's core. Geomagn. Aeron. (USSR), 7: 1050. Translated in Geomagn. Aeron., 7: 851–859 (1967).

Busse, F.H., 1970. Thermal instabilities in rapidly rotating systems. J. Fluid Mech., 44: 441–460.

Busse, F.H., 1973. Generation of magnetic fields by convection. J. Fluid Mech., 57: 529–544.

Busse, F.H., 1975. A model of the Geodynamo. Geophys. J.R. Astron. Soc., 42: 437–459.

Busse, F.H., 1976. Generation of planetary magnetism by convection. Phys. Earth Planet. Inter., 12: 350–358.

Busse, F.H., 1978a. Theory of Planetary dynamos. In: C.F. Kennel, L.J. Lanzarotti and E.N. Parker (Editors), Solar System Plasma Physics.

Busse, F.H., 1978b. Introduction to the theory of geomagnetism. In: P.H. Roberts and A.M. Soward (Editors), Rotating Fluids in Geophysics, Academic Press, London, pp. 361–388.

Busse, F.H. 1978c. Magnetohydrodynamics of the Earth's dynamo. Ann. Rev. Fluid. Mech., 10: 435–462.

Chandrasekhar, S., 1961. Hydrodynamic and Hydromagnetic Instability. Oxford University Press, Oxford.

Childress, S., 1976. Convective dynamos. Springer Lecture Notes in Physics, 71: 195–224.

Childress, S. and Soward, A.M., 1972. Convection-driven hydromagnetic dynamos. Phys. Rev. Lett., 29: 837–839.

Eltayeb, I.A., 1972. Hydromagnetic convection in a rapidly rotating fluid layer. Proc. R. Soc. London, Ser. A, 326: 229–254.

Eltayeb, I.A., 1975. Overstable hydromagnetic convection in a rotating layer. J. Fluid Mech., 71: 161–179.

Eltayeb, I.A. and Kumar, S., 1977. Hydromagnetic convective instability of a rotating, self gravitating fluid sphere containing a uniform distribution of heat sources. Proc. R. Soc. London, Ser. A, 353: 145–162.

Fearn, D.R., 1979a. Thermally driven hydromagnetic convection in a rapidly rotating sphere. Proc. R. Soc. London, in press.

Fearn, D.R., 1979b. Thermally and magnetically driven instabilities in a rapidly rotating sphere. Geophys. Astrophys. Fluid Dyn., in press.

Loper, D.E., 1975. Torque balance and energy budget for the precessionally driven dynamo. Phys. Earth Planet. Inter., 11: 43–60.

Moffatt, H.K., 1978. Generation of Magnetic Fields by Electrically Conducting Fluids. Cambridge University Press, Cambridge.

Roberts, P.H., 1968. On the thermal instability of a rotating fluid sphere containing heat sources. Philos. Trans. R. Soc. London, Ser. A, 263: 93–117.

Roberts, P.H., 1978. Magneto-convection in a rapidly rotating fluid. In: P.H. Roberts and A.M. Soward (Editors), Rotating Fluids in Geophysics, Academic Press, London, pp. 420–436.

Roberts, P.H. and Loper, D.E., 1979. On the diffusive instability of some simple steady magnetohydrodynamic flows. J. Fluid Mech., 90: 641–668.

Roberts, P.H. and Stewartson, K., 1974. On finite amplitude convection in a rotating magnetic system. Philos. Trans. R. Soc. London, Ser. A, 277: 287–315.

Roberts, P.H. and Stewartson, K., 1975. Double roll convection in a rotating magnetic system. J. Fluid Mech., 68: 447–466.

Rochester, M.G., Jacobs, J.A., Smylie, D.E. and Chong, K.F., 1975. Can precession power the geomagnetic dynamo? Geophys. J. R. Astron. Soc., 43: 661–678.

Soward, A.M., 1974. A convection-driven dynamo I. The weak field case. Philos. Trans. R. Soc. London, Ser. A, 275: 611–651.

Soward, A.M., 1977. On the finite amplitude thermal instability of a rapidly rotating fluid sphere. Geophys. Astrophys. Fluid Dyn., 9: 19–74.

Soward, A.M., 1978. The kinematic dynamo problem. In: P.H. Roberts and A.M. Soward (Editors), Rotating Fluids in Geophysics, Academic Press, London, pp. 351–359.

Soward, A.M., 1979a. Thermal and magnetically driven convection in a rapidly rotating fluid layer. J. Fluid Mech., 90: 669–684.

Soward, A.M., 1979b. Finite amplitude thermal convection and geostrophic flow in a rotating magnetic system. J. Fluid Mech., in press.